© 2021 Wiley-VCH GmbH.

ADVANCED HEALTHCARE MATERIALS

Supporting Information

for *Adv. Healthcare Mater.*, DOI: 10.1002/adhm.202002103

Fast stereolithography printing of large-scale biocompatible hydrogel models

Nanditha Anandakrishnan [a,#], Hang Ye [b,#], Zipeng Guo [b,#], Zhaowei Chen [a], Kyle I. Mentkowski [a,c], Jennifer K. Lang [a,c,d], Nika Rajabian [e], Stelios T. Andreadis [a,e], Zhen Ma [f], Joseph A. Spernyak [g], Jonathan F. Lovell [a], Depeng Wang [a], Jun Xia [a], Chi Zhou [b,], Ruogang Zhao [a]*

Supporting Information

Fast stereolithography printing of large-scale biocompatible hydrogel models

Nanditha Anandakrishnan [a,#], Hang Ye [b,#], Zipeng Guo [b,#], Zhaowei Chen [a], Kyle I. Mentkowski [a,c], Jennifer K. Lang [a,c,d], Nika Rajabian [e], Stelios T. Andreadis [a,e], Zhen Ma [f], Joseph A. Spernyak [g], Jonathan F. Lovell [a], Depeng Wang [a], Jun Xia [a], Chi Zhou [b,], Ruogang Zhao [a,*]*

Supplementary Tables

Table S1. A list of hydrogel material composition for all printed parts

Description of Printed part	Polymer concentration	LAP concentration	Photoabsorber concentration	Comments	Figure
Liquid flow velocity measurement	20% PEGDA, 80% PEGDA 400 Da	0.60%	0.03% Orange G	Flow fluorescent microbeads (d = 25 μm)	Figure 1D
Suction force measurement	10 % PEGDA, 20% PEGDA 400 Da	0.60%	No photoabsorber used		Figure 1E
FLOAT-printed cube	20% PEGDA 4k Da	0.60%	0.1% Quinoline yellow		Figure 1F
FLOAT-printed hand model with or without vascular channels	10% PEGDA 400 Da	1%	0.06% Quinoline yellow		Figure 3A-G
Effect of photoabsorbers on cured depth and printing resolution	20% PEGDA 4k Da	0.60%	Varies		Figure 2A-C
A FLOAT-printed vascular tree structure on a rectangular PEGDA slab	20% PEGDA 4k Da	0.60%	0.2% Quinoline yellow		Figure 2D
A FLOAT-printed array of human hand models, a truss and primitives	20% PEGDA 4k Da	0.60%	0.2% Quinoline yellow		Figure 2F-G
FLOAT-printed acellular liver model	15% PEGDA 4k Da	0.60%	0.15% Quinoline yellow		Figure 4A-C, Figure S14
Hydrogel stiffness measurement	Varies	0.60%	No photoabsorber used		Figure S5
Cell-laden gyroid model	7% GelMA plus 3% PEGDA	0.60%	0.06% Quinoline yellow	Osteogenic differentiation of the hMSCs	Figure S11
Study of printing induced cell injury	7% GelMA + 2% PEGDA 8k Da	0.60%	0.015% Quinoline yellow	Cardiomyocytes, hiPSC-MSCs and hSMCs were encapsulated at a density 2 x 10^6 cells per mL	Figure 3H-I
FLOAT-printed cell-laden liver model with and without interconnected vasculature	15% PEGDA 4k Da + 10 mM a-PEG-RGD	0.60%	0.15% Quinoline yellow	8 x 10^6 HepG2 cells per mL encapsulated	Figure 4E-G
Endothelialization of printed channels in hydrogel tissue model	7% GelMA + 3% PEGDA 8 kDa	0.60%	0.015% Quinoline yellow		Figure 5A-F
Diffusional permeability of printed channels	7% GelMA + 3% PEGDA 8 kDa	0.60%	0.015% Quinoline yellow		Figure 5G-I
Degradable material printing	5% 8-arm PEG norbornene plus 8% GelMA	0.6%	No photoabsorber		Figure S6

Table S2. A list of printed parts with cells

Figure	Description of the model	Material composition	Cell type	Cell density	Culture time	Characterization method
Figure 3H-I	Effect of FLOAT printing on cellular metabolic activity and cytotoxicity. Solid hydrogel part (3 mm*3mm*2 cm).	7% GelMA + 2% PEGDA 8K Da, 0.6% LAP, 0.015% Quinoline yellow	Cardiomyocytes isolated from neonatal mouse hearts, human induced pluripotent stem cells derived mesenchymal stem cells (hiPSC-MSCs) and human skeletal muscle cells (hSMCs)	2 x 10^6 cells per mL	2 hours	XTT viability assay (Colorimetric) and Lactate dehydrogenase (LDH) release assay (Colorimetric)
Figure 4E-G	FLOAT-printed cell-laden liver model with and without interconnected vasculature	15% PEGDA 4K Da + 10 mM a-PEG-RGD, 0.6% LAP, 0.15% Quinoline yellow	HepG2 cells	8 x 10^6 cells per mL	3 days, perfusion culture	Live/Dead viability assay (L-3224, Thermo Fisher)
Figure 4H	Albumin production in 3D printed liver models	8% GelMA + 5% PEGDA, 0.6% LAP, 0.015% Quinoline yellow	HepG2 cells and normal human dermal fibroblasts	8 x 10^6 cells per mL	6 days, perfusion culture	Human Albumin ELISA, Abcam
Figure 5A-F, Figure S15	Endothelialization of printed channels in hydrogel tissue model	7% GelMA + 3% PEGDA 8 kDa, 0.6% LAP, 0.015% Quinoline yellow	RFP tagged Human umbilical vein endothelial cells (HUVECs)	10 x 10^6 cells per mL	9 days	Immunofluorescence staining, Confocal Microscopy
Figure 5G-I	Diffusional permeability of printed channels	7% GelMA + 3% PEGDA 8 kDa, 0.6% LAP, 0.015% Quinoline yellow	RFP tagged Human umbilical vein endothelial cells (HUVECs)	10 x 10^6 cells per mL	9 days	FITC- Dextran injected into channels and its diffusion was characterized using Fluorescence microscopy
Figure S S11A-B	FLOAT printed Gyroid model (2cm*2cm*2cm)	7% GelMA + 3% PEGDA 8 kDa, 0.6% LAP, 0.06 % Quinoline yellow	Human mesenchymal stem cells (hMSCs)	5 x 10^6 cells per mL	9 days	Live/Dead viability assay (L-3224, Thermo Fisher)
Figure S S11C	Osteogenic differentiation of hMSCs encapsulated in FLOAT printed gyroid model	7% GelMA + 3% PEGDA 8 kDa, 0.6% LAP, 0.06 % Quinoline yellow	Human mesenchymal stem cells (hMSCs)	5 x 10^6 cells per mL	9 days (8 days in osteogenic differentiation media)	Alkaline phosphatase (ALP) activity using Fast Blue RR Salt/Napthol (Sigma)
Figure S S12	Effect of 3D printing process on the uniformity of cell distribution (Part dimension: 8*8*20 mm)	10% PEGDA 4000 Da, 0.6% LAP, 0.02% Quinoline yellow	Human skeletal muscle cells (hSMCs)	5 x 10^6 cells per mL	Imaged immediately after printing	Calcein AM staining
Figure S S13	High cell density printing demonstration using FLOAT (Part dimension: 5*5*10 mm)	10% PEGDA 4000 Da, 0.6% LAP, 0.02% Quinoline yellow	3T3 fibroblasts	50 million cells per mL	Imaged immediately after printing	Calcein AM staining

Supplementary Figures

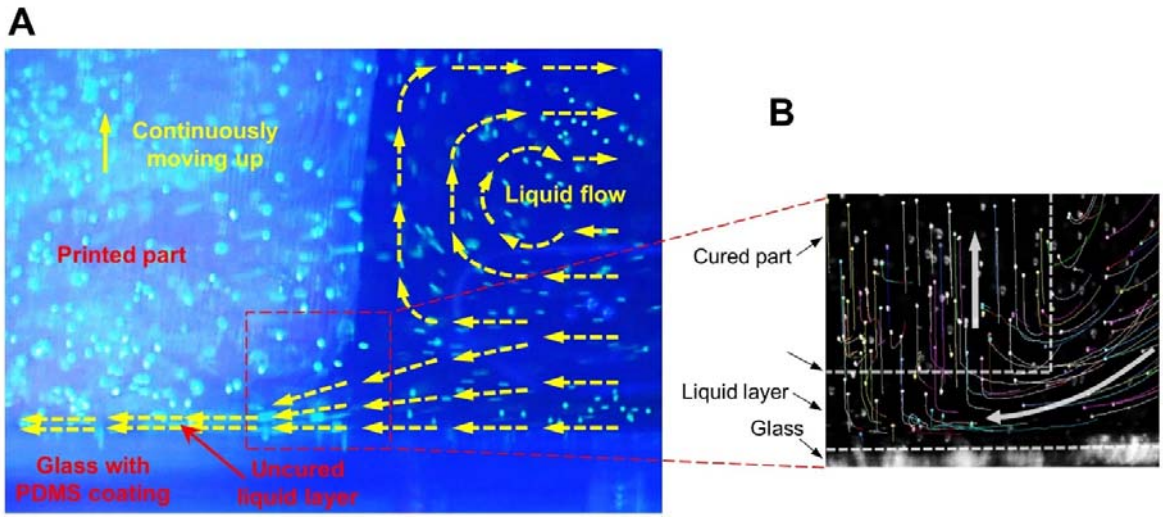

Figure S1. (A) An experimental image showing the liquid-solid interface in FLOAT printing. Fluorescence microbeads were added in the prepolymer solution to aid the analysis of the liquid flow direction and velocity. Trajectory lines were added manually to illustrate the flow direction of the liquid. (B) Computer-tracked trajectories of fluorescence microbeads showing the prepolymer liquid flow during printing.

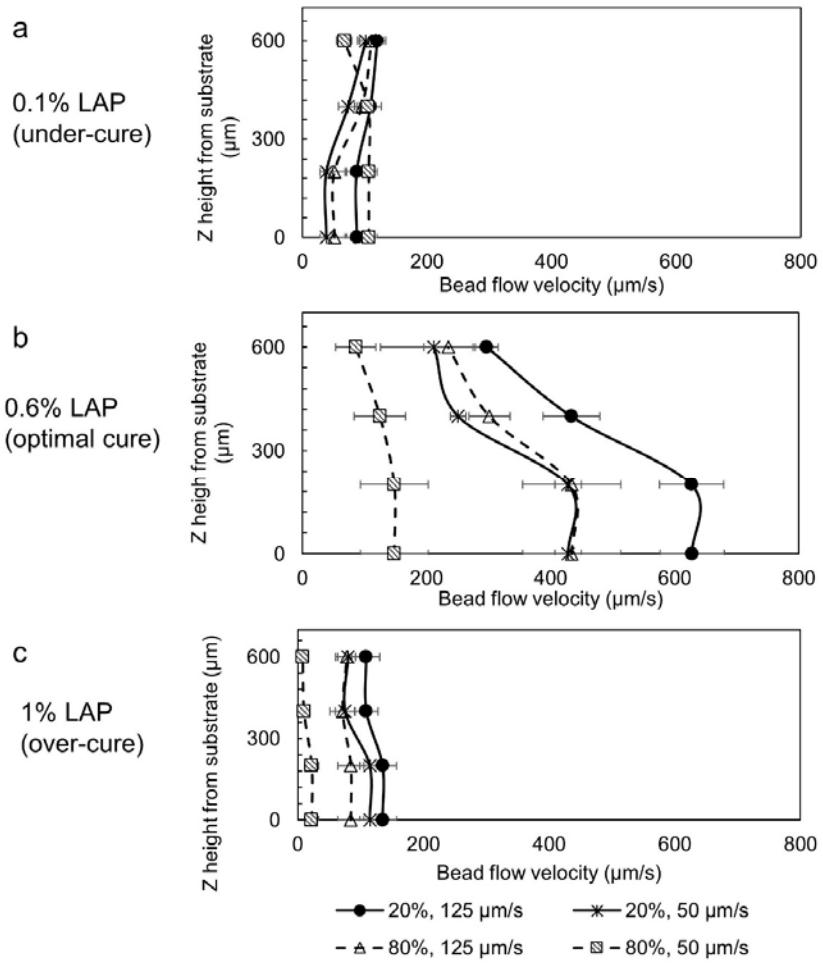

Figure S2. The flow velocity profile of PEGDA prepolymer solution under different photo-curing conditions. The measurement was performed by tracking the motion of the fluorescence microbeads in the photopolymerization zone just beneath the cured part. (A) Low photoinitiator concentration (0.1% LAP) results in undercured condition. The lack of photopolymerization greatly reduced the need for precursor material replenishment. As a result, only low-velocity, random and localized bead flow was observed. (B) In optimally cured condition (0.6% LAP), measured liquid flow velocity is in the order of several hundred micrometers per second and the highest flow velocity was observed in low concentration solution (20% PEGDA) under high printing speed (125 μm/s), while the lowest flow velocity was observed in high concentration solution (80% PEGDA) under low printing speed (50 μm/s). (C) High photoinitiator concentration (1% LAP) results in over-cured condition. In this case, fast photopolymerization results in the formation of a thin layer (1 - 2 mm thick) at the tank bottom that interferes with prepolymer flow. As a result, only low-velocity bead flow was observed.

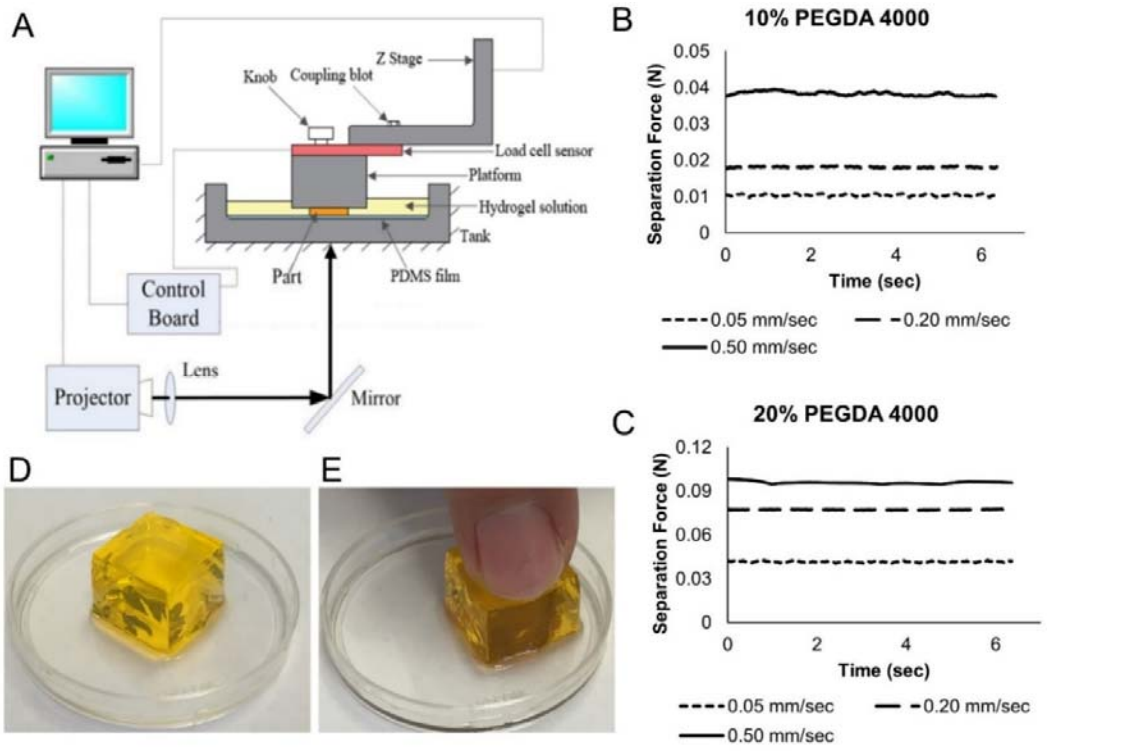

Figure S3. (A) Experimental setup for fluid suction force measurement. A force sensor was installed between the platform and the Z stage and was used to report the suction force between the cured part and the tank base. Experimentally measured suction forces during FLOAT printing of 10% PEGDA (B) and 20% PEGDA (C) under different printing speeds. Note the suction forces maintain at a constant value during the FLOAT printing, indicating a stable printing process. (D) FLOAT-printed PEGDA cube of 1 cm edge length. Note the smooth surface and sharp edges of the hydrogel cube as a result of the stable printing process of the FLOAT. (E) PEGDA cube is very soft and can be easily deformed by finger compression.

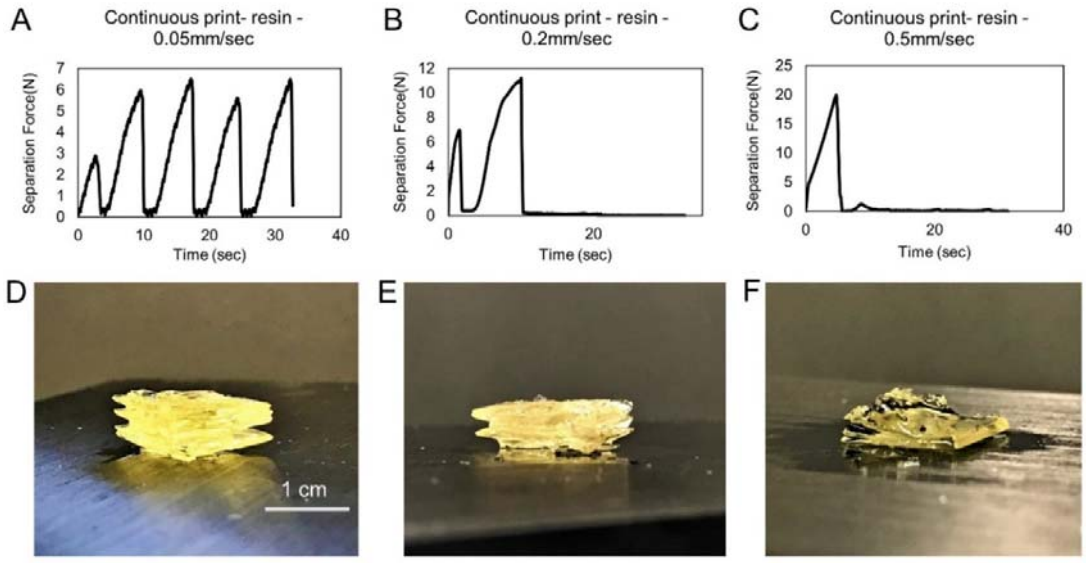

Figure S4. (A-C) Experimentally measured suction forces during continuous SLA printing of acrylic resin at various printing speeds. (D-F) Images of corresponding resin parts printed during suction force measurement. In panel (A), the highly wavy curve of the suction force at low printing speed (0.05 mm/s) indicates an unstable printing process which results in obvious delamination in the printed part (D). Note the number of peaks (4) in the suction force curve roughly matches the number of delaminated layers (3-4) in the part, suggesting the peak force occurs when the layer is attached to substrate and zero force (trough) occurs when the layer suddenly detaches from the substrate. In panels (B) and (C), only 1-2 force peaks were recorded, which correspond to 1-2 layers in the printed parts (E, F). The premature failure of the parts under these higher printing speeds (0.2 and 0.5 mm/s) is due to the very high suction forces that cause damage to the PDMS coating on the glass substrate.

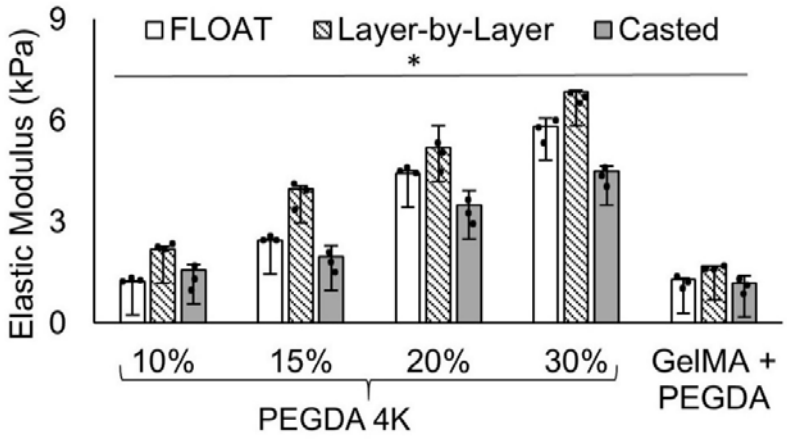

Figure S5. The stiffness of FLOAT-printed PEGDA and composite hydrogels compared to that of layer-by-layer printed and casted hydrogels. Data are reported as the mean ± SD. n = 3; *, $p < 0.001$ determined by one-way ANOVA test.

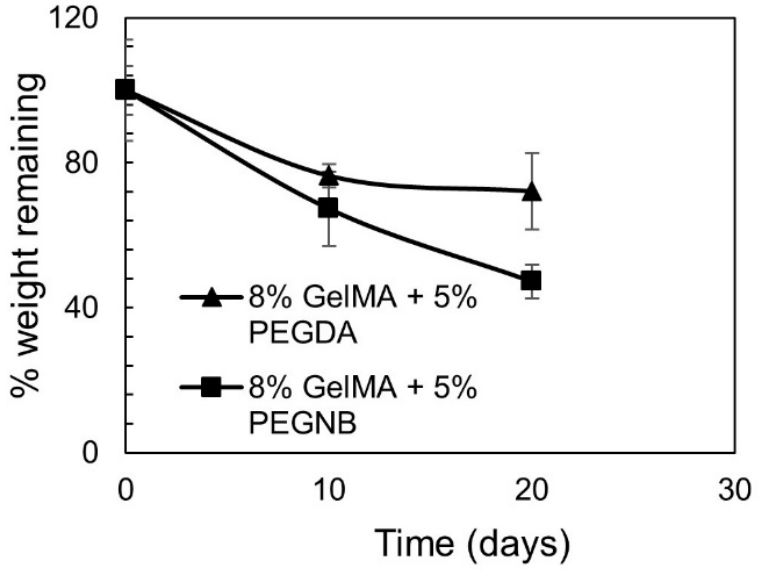

Figure S6. Demonstration of the ability of the FLOAT method to print biodegradable materials. FLOAT was sued to print a composite hydrogel scaffold composed of 8% GelMA blended with 5% 8-arm PEG norbornene (PEGNB), which is hydrolytically degradable. 51% dry weight reduction in GelMA/PEGNB scaffold and 28% dry weight reduction in GelMA/PEGDA scaffold were observed after 20 days incubation in PBS.

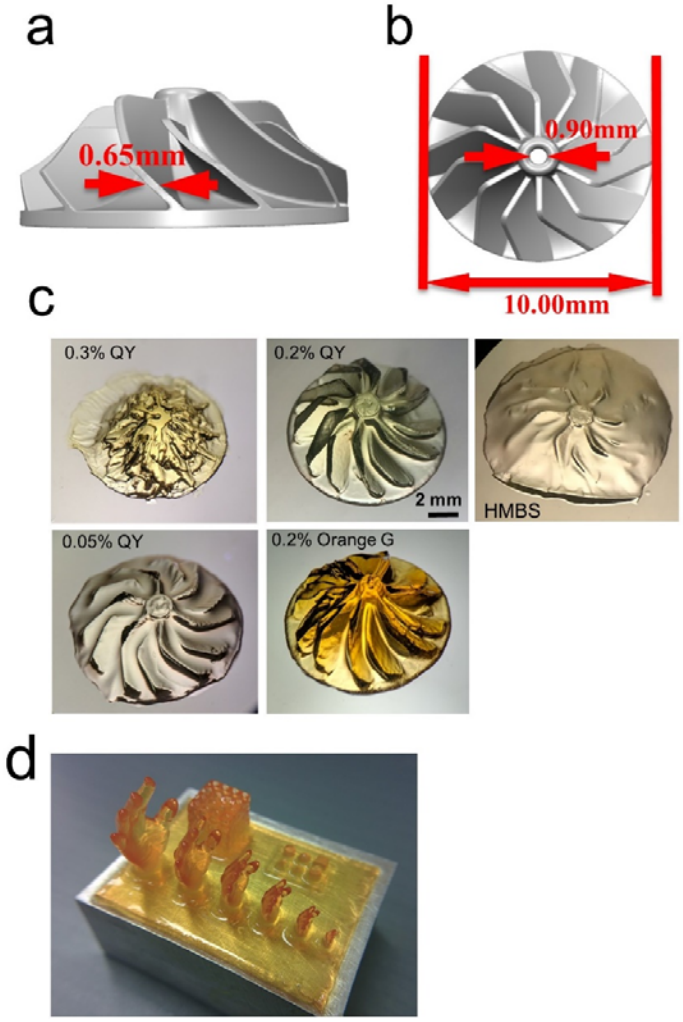

Figure S7. (A-B) Sideview and topview of the digital turbine rotor model with dimensions. (C) Pictures of printed turbine rotor models using optimal photoabsorber setting (0.2% QY) and HMBS. (D) FLOAT-printed PEGDA human hand models, a truss model and primitives viewed from hand model side. The base slab is 3.5 cm x 2.5 cm.

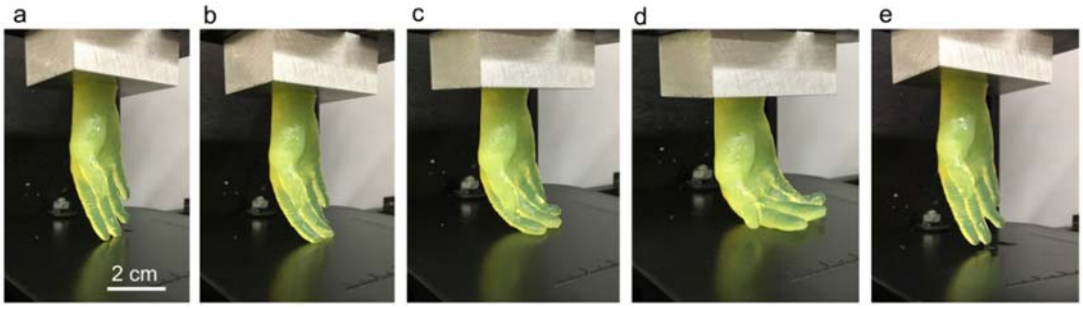

Figure S8. FLOAT-printed PEGDA human hand model under compression. (a-d) Sequential images show gradually increased bending of fingers under compression. (e) Recovery of the fingers upon compression release.

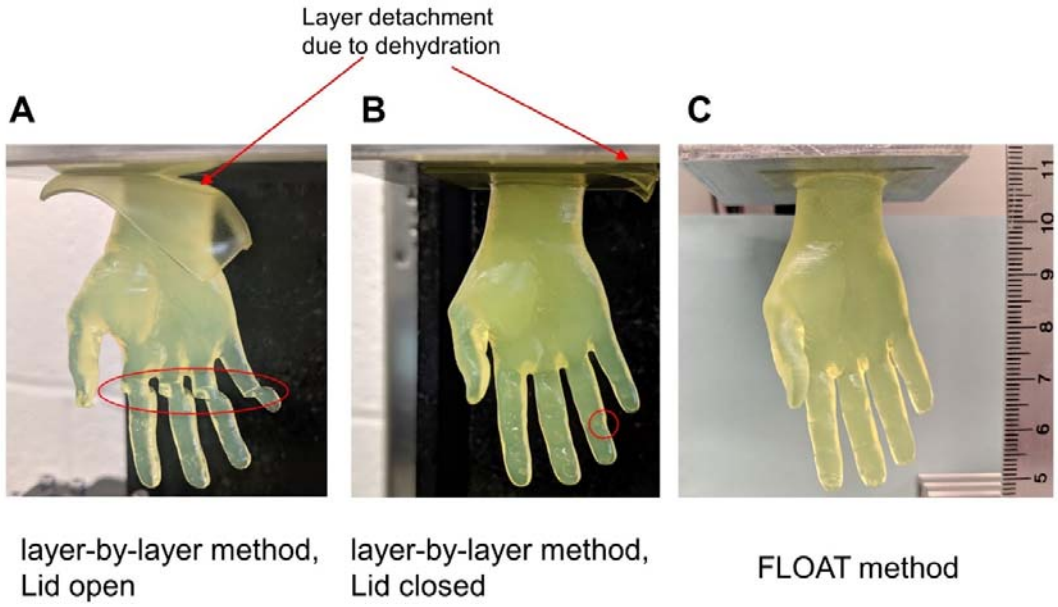

Figure S9. Comparison on the quality of a centimeter-sized hydrogel hand model printed using a traditional layer-by-layer based SLA method and FLOAT method. It took 2 hours to print the hand model using the traditional layer-by-layer based SLA process at 150 μm layer thickness. During this process, hydrogel dehydration occurred, causing layer detachment from the platform and misalignment in the fingers (red circles). (A) Hand model printed with printer lid open (rapid dehydration), severe layer detachment can be seen, which caused severe misalignment in the fingers. (B) Hand model printed with printer lid closed (slow dehydration). Mild layer detachment and finger misalignment can be seen. (C) Hand model is printed using FLOAT method in 19 mins. No dehydration is observed.

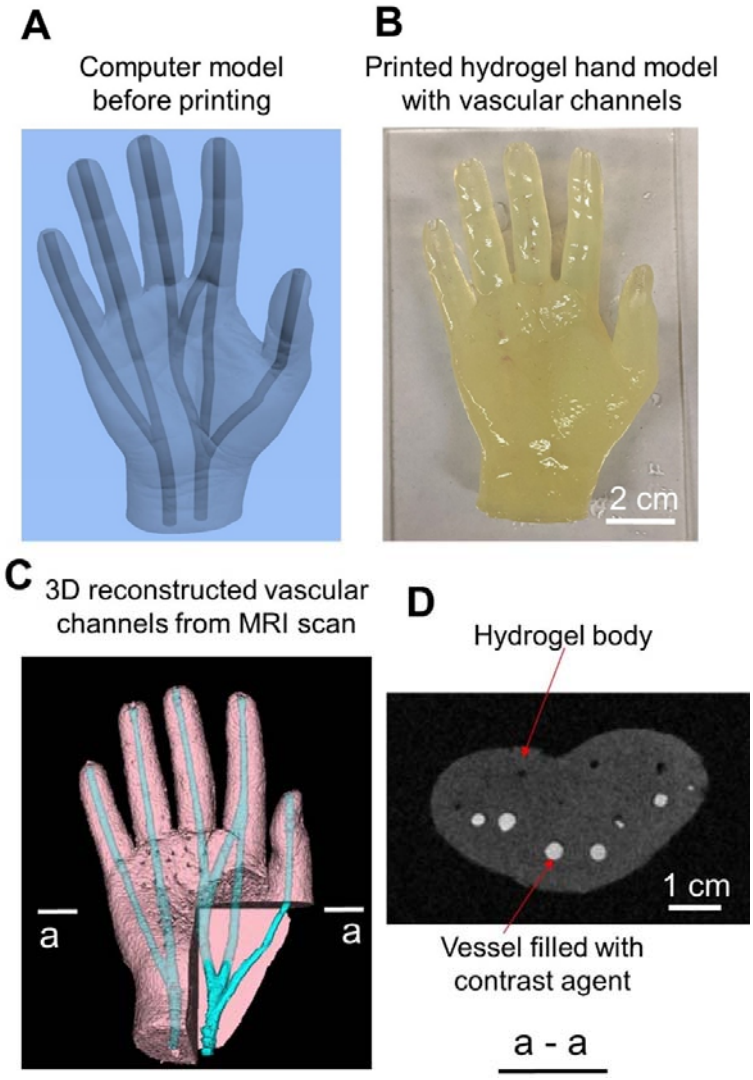

Figure S10. A centimeter-sized human hand model containing perfusable vascular channels. (A) Computer generated model before printing. (B) Hand model printed by the FLOAT method. (C) 3D reconstructed image of the hand model from MRI scanning. The channels are visualized with the aid of mineral oil as a contrast agent. (D) MRI cross-sectional view of the hand model at the palm region ('a-a' cross-section). Contrast agent filled vessels are visible.

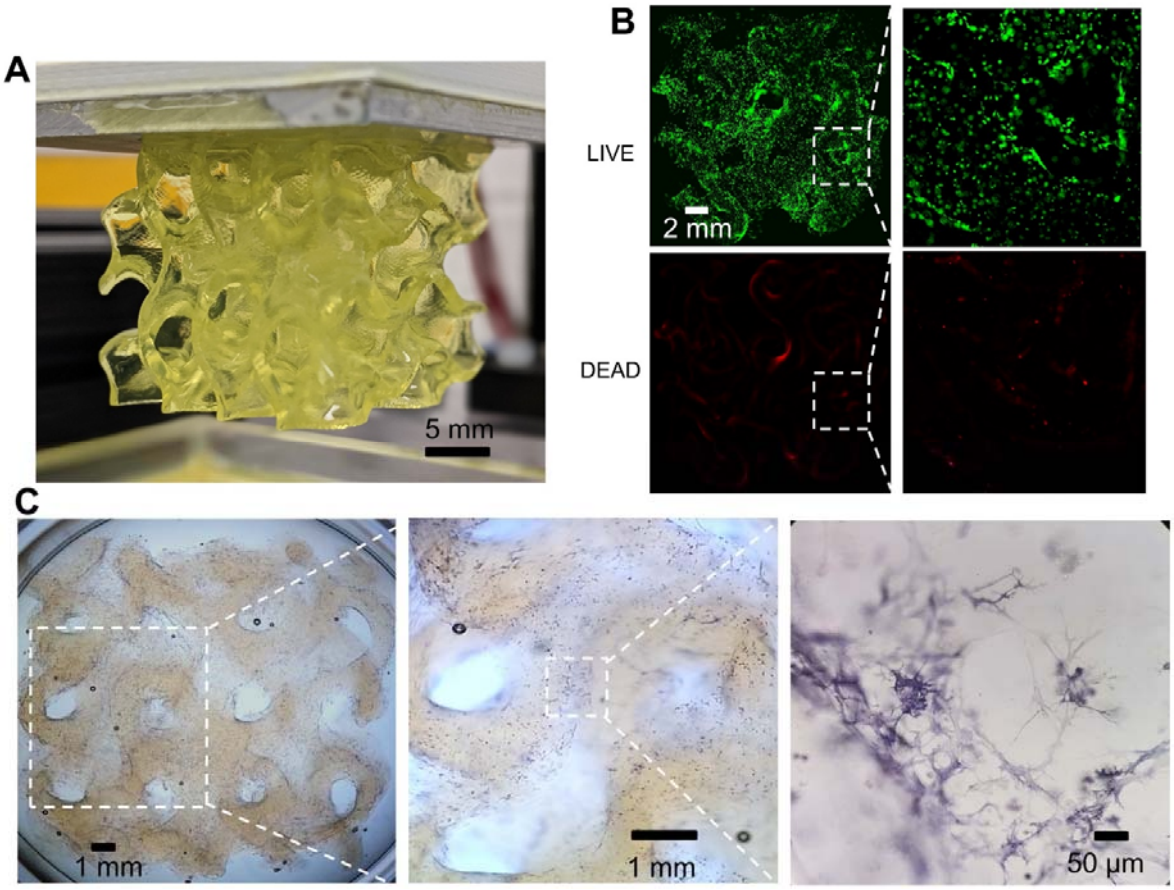

Figure S11. (a) A FLOAT-printed gyroid model with encapsulated human mesenchymal stem cells (hMSCs). (b) Live/Dead staining of the thin slice of the gyroid model showing majority of the encapsulated cells are viable after 9 day culture. (c) The positive ALP staining of the thin slice of the gyroid model showing the hMSCs spread well and undergo osteogenic differentiation during a 9 day culture period.

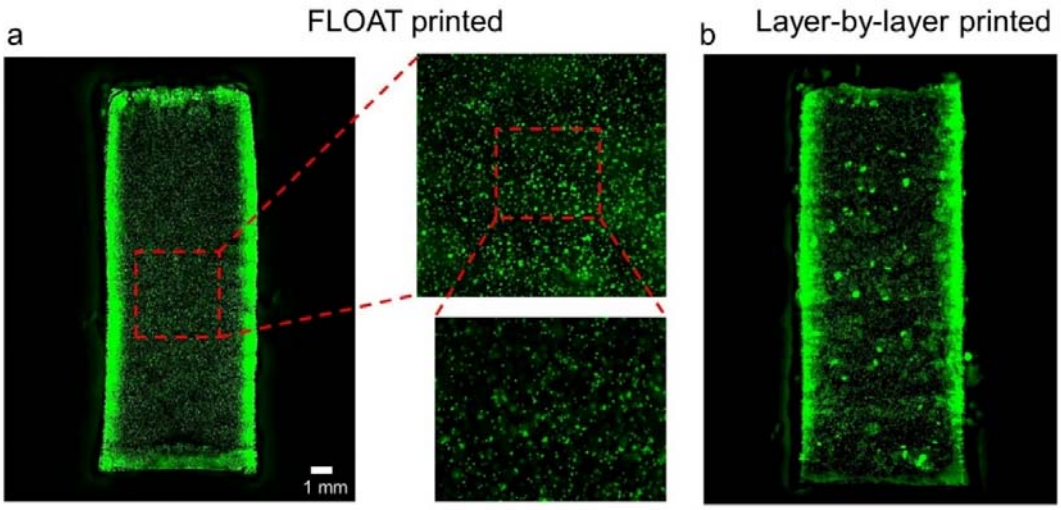

Figure S12. (a) Demonstration of the cell uniformity in FLOAT-printed centimeter-sized hydrogel part. The part size is 8*8*20 mm. The part was printed (platform moving direction) along its long axis. It took 6 mins to print this part. (b) Non-uniform cell distribution is seen in layer-by-layer printed part of the same size. Prepolymer solution containing cells was manually pipetted once in a while to prevent cell settling; however, layered cell distribution and cell aggregates were still seen in the part. It took 2 hours to print this part. Human skeletal muscle cells are used in both models.

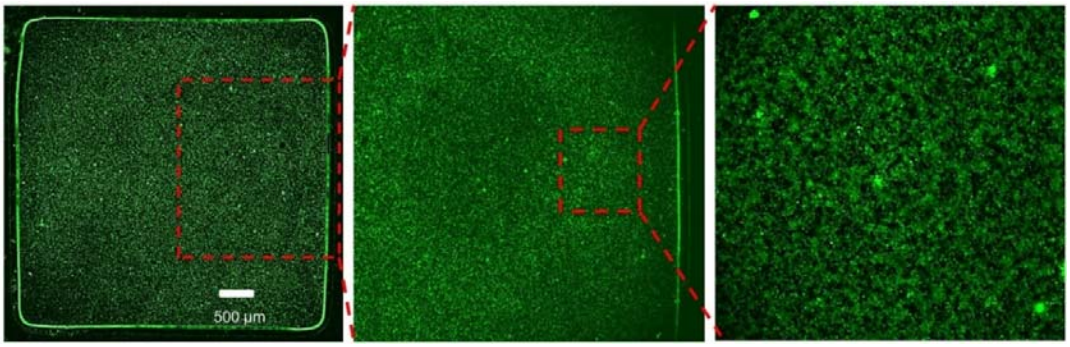

Figure S13. Demonstration of the ability of the FLOAT method to print at high cell density. Images show a centimeter-sized hydrogel part of 5*5*10 mm printed with 3T3 cells at a density of 50 million cells per mL.

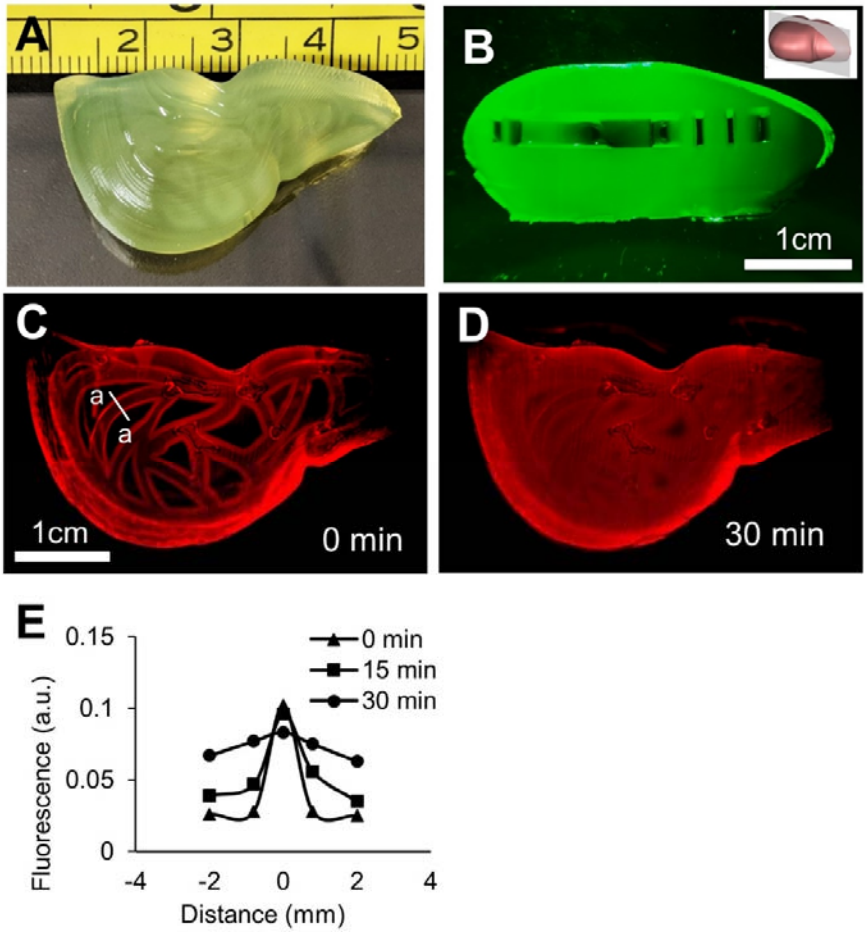

Figure S14. FLOAT printing of a centimeter-scale hydrogel liver model containing perfusable channels. (A) A liver model with smooth surface and monolithic, translucent hydrogel body was printed using 15% PEGDA 4 kDa. Measuring tape unit is in centimeter. (B) Cross-sectional view of the liver model to show the channel openings. Inset shows the direction of the cut. (C) Beginning of Rhodamine B dye diffusion. (D) Full diffusion of the dye into the interstitial space of the liver model was achieved 30 minutes after injection. (E) A representative plot of the fluorescence intensity change due to dye diffusion in the vicinity of a vascular channel (a-a cross-section shown in panel C) over a 30 minute period.

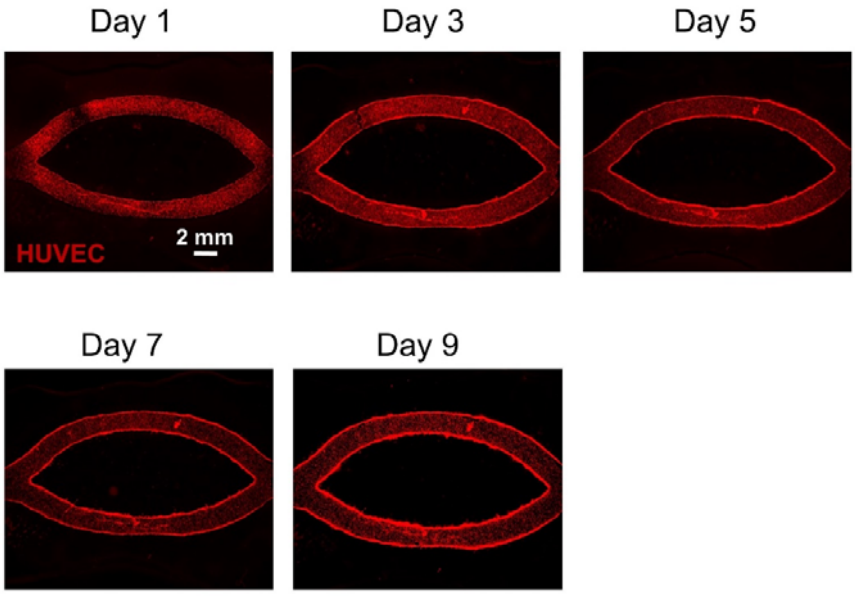

Figure S15. Time-lapsed images show the HUVEC coverage in printed channels in a hydrogel part. In the first three days after seeding, HUVEC coverage was found to be uniform in the channels except for a couple of isolated gaps. A uniform and confluent layer of endothelial cells formed after day 3 and remained stable up to day 9. This hydrogel model containing channels was printed using 7% GelMA + 3% PEGDA 8000.

Other supplementary materials for this manuscript include the following:

Movie S1. Motion of the fluorescence microbeads demonstrates the flow dynamics of the hydrogel prepolymer during FLOAT printing of a centimeter-sized, solid part. This FLOAT printing is performed under an optimal photo-curing condition (0.6% LAP). The bright object in the center is the building platform where the part attaches to. As the platform started to move up, microbeads were first carried by the flow into a liquid layer underneath the curing part, then trapped in the hydrogel upon photocuring and carried upwards by the cured part. As a result, continuous replenishment of prepolymer solution below the curing part was achieved, which supports nonstop part growth.

Movie S2. Tracked trajectories to show the motion of fluorescence microbeads during FLOAT printing under an optimal photo-curing condition (0.6% LAP). As the curing part started to move up, microbeads were first carried by the flow into a liquid layer underneath the curing part, then trapped in the hydrogel upon photocuring and carried upwards by the cured part.

Movie S3. Motion of the fluorescence microbeads demonstrates the prepolymer flow dynamics under over-cured condition (high photoinitiator concentration, 1% LAP). In this case, fast photopolymerization results in the formation of a thin layer (1 - 2 mm thick) at the tank bottom that interferes with prepolymer flow. Since the printing platform continuously moves up, it pulls on the thin layer, causing the layer to detach from the tank bottom. The layer detachment results in the sudden influx/filling of precursor material that is then rapidly photopolymerized into a solid layer attaching to the tank bottom. This attachment-detachment process cycles through the rest of the printing period. As a result, the uniformity and the surface finishing of the printed part is greatly compromised.

Movie S4. FLOAT printing of a centimeter-size PEGDA human hand model. A timer is places to the left of tank to show real printing time. As the printing starts, curing light is projected into the tank to initiate photo-polymerization, and the platform moves continuously to draw the hand model out of the liquid pool. The entire printing process lasts for 20 minutes. The hand model is 2.6 cm x 1.7 x 5.6 cm. The printing was performed in a deep tank to help maintaining the surface smoothness of the printed part. It would take 6.5 hours to print the same model using traditional layer-by-layer based SLA process.

Movie S5. Compression test of the centimeter-size human hand model. The hand model is very compliant, as demonstrated by gradually increased bending of fingers under compression. Finger bending fully recovered upon compression release.

Movie S6. FLOAT printing of a centimeter-size PEGDA liver model. In the beginning, build platform is partially submerged in the tank that contains PEGDA prepolymer. A timer is places to the left of tank to show real printing time. As the printing starts, blue curing light is projected into the tank to initiate photo-polymerization, and the platform moves continuously to draw the liver model out of the liquid pool. The entire printing process lasts for 4.45 minutes. The liver model is 3.5 cm x 2.5 cm x 1.5 cm.

Movie S7. Rhodamine dye injection into the pre-fabricated channel network of FLOAT-printed PEGDA liver model.